UNIVERSITY OF LATVIA
FACULTY OF BIOLOGY
DEPARTMENT OF MOLECULAR BIOLOGT

SUBCUTANEOUS CANINE AND FELINE NEOPLASM *EX VIVO* CHARACTERIZATION USING RAMAN SPECTROSCOPY

BACHELOR THESIS

Author: Mikus Melderis
Student's card No. mm14067
Supervisor: Dr.phys Mindaugas Tamošiūnas
Reviewer: Dr.phys Blaz Cugmas

RIGA 2021

Abstract

As cancer is one of the leading causes of death in both humans and animal companions a development of a fast, cost-effective and non-invasive detection and diagnostics method is of great importance. Raman spectroscopy is a non-invasive optical technique capable of fulfilling this role. The main goal of this study was to obtain Raman spectra from feline and canine tumour and skin samples *ex vivo*, to characterize them and to evaluate the ability to differentiate between tumour and skin tissue samples as a possible tool in cancer diagnosis in the near infrared region (300 to 950 cm^{-1}). The study used 4 mast cell tumour, 9 soft tissue sarcomas and 27 skin tissue samples, preserved in 10% formalin solution. Tissue sample Raman spectra characterization showed significant similarities between the samples, with cholesterol-related Raman peaks at 445, 538, 548, 614 and 702 cm^{-1}. The tumour tissues were detected with sensitivity and specificity of 57.1% and 80.7%, respectively, and with 72.5% accuracy. The results show that the selected Raman spectral region is not suitable for the characterization of canine and feline tumour and skin tissues as other regions have been shown to have higher detection results.

Key words: Raman spectroscopy, soft tissue sarcoma, skin tumours, mast cell tumours, diagnosis

Kopsavilkums

Vēzis ir viens no galvenajiem cilvēku un mājdzīvnieku nāves cēloņiem. Tādēļ liela nozīme ir ātras, rentablas un neinvazīvas diagnostikas metodes izstrādei. Ramana spektroskopija ir neinvazīva optiskā metode, kas derētu šādam mērķim. Šī pētījuma galvenais uzdevums bija iegūt Raman spektrus no kaķu un suņu audzējiem un ādas paraugiem *ex vivo,* tos raksturot, un atšķirt audzēja un ādas audu paraugus tuvu infrasarkanās gaismas reģionā (300 līdz 950 cm^{-1}). Pētījumā tika izmantoti 4 tuklo šūnu audzēji, 9 mīksto audu sarkomas un 27 ādas audu paraugi, uzglabāti 10% formalīna šķīdumā. Audu paraugu Ramana spektru raksturojums parādīja būtisku līdzību starp paraugiem, ar holesterīnu saistītās Ramana joslās pie 445, 538, 548, 614 un 702 cm^{-1}. Audzēja audi tika klasificēti ar jutīgumu un specifiskumu attiecīgi 57,1% un 80,7% un ar 72,5% precizitāti. Rezultāti parāda, ka izvēlētais Ramana spektrālais reģions nav piemērots suņu un kaķu audzēju un ādas audu raksturošanai, jo ir parādīts, ka citiem reģioniem ir augstāki klasificēšanas rezultāti.

Atslēgas vārdi: Ramana spektroskopija, mīksto audu sarkoma, ādas audzēji, tuklo šūnu audzēji, diagnostika

Table of contents

List of abbreviations

MCT- mast cell tumour

STS – soft tissue sarcoma

BCC – basal cell carcinoma

cm^{-1} – inverse centimetre

°C – degree Celsius

SCC – squamous cell carcinoma

C=O – carbon oxygen double bond

C-N – carbon nitrogen bond

C-C – carbon carbon bond

nm - nanometre

CCD – charge-coupled device

mm - millimetre

PC – principal component

PCA – principal component analysis

TN – true negative

FN – false negative

FP – false positive

TP – true positive

INTRODUCTION

Cancer is a very common cause of animal companion deaths, in fact, the leading cause of deaths in canines is cancer, as around 50% of geriatric dogs and 33% of cats dying from cancer. According to several studies, the number of tumours originating from the skin or directly underneath the skin is in a range between 25 to 50% [1,2]. The most common approach for cancer detection is based on biopsies. However, the method is painful, and animals might require sedation, it has to be performed several times to avoid false negative results. In addition, the experience of the veterinarian has a very significant impact on the procedure and its accuracy, which for untrained personnel can vary due to tumours heterogeneous structure and other peculiarities [1,3].

Raman spectroscopy would offer a non-invasive method for benign and malignant tumour detection, that would also be cost-effective and easy to perform. Studies focusing on near infrared region are few and thus it provides a promising tool for cancer diagnosis in pets and possibly also in comparative oncology.

The main goal of this study was to obtain Raman spectra from feline and canine tumour and skin samples ex vivo, to characterize them and to evaluate the ability to differentiate between tumour and skin tissue samples as a possible tool in cancer diagnosis in the near infrared region (300 to 950 cm^{-1}).

To achieve this goal following tasks were set

- To collect Raman spectra from the tissue samples
- Analyse and characterize the obtained spectra
- Test and evaluate the accuracy with which the sample are distinguished and compare with other spectral regions

The study was carried out at the Institute of Atomic Physics and Spectroscopy / Biophotonics Laboratory of the University of Latvia within the project “Multimodal imaging for veterinary oncology using a combination of optical coherence tomography and photoacoustic microscopy”

1. LITERATURE REVIEW

1.1.Raman spectroscopy

Raman spectroscopy is a molecular spectroscopic method, which uses the interaction between the light and the molecules making up the sample, to obtain information about the sample's molecular make-up or specific characteristics, the samples can be solid, liquid, gases, aerosols and vapours and the measurements can be done in temperatures ranging from well below zero to several hundred °C. for solid sample analysis little if any at all, sample preparation is required, as for liquids, a glass or plastic container is sufficient, to obtain results [4]. This is achieved by sending a beam of photons through the sample and a process called Raman scattering, named after Sir C.V. Raman, who was the first to describe it [5].

When light interacts and is scattered by a molecule, the electromagnetic field of a photon causes polarization of the electrons in the molecule, the energy is transferred from the photon to the molecule [5]. This can be treated as a new virtual state or level of the molecule, as it is very short-lasting because the photon is reemitted near instantaneously, simply as scattered light. In the vast majority of cases of scattering the energy of the molecule remains the same, as it was before, and the energy and wavelength of both the photon and the molecule remain the same. This process is called elastic or Rayleigh scattering [6].

However, in around 1 photon in 10 million, instead inelastic or Raman scattering occurs, where the energy is transferred between the scattered photon and the molecule. This can happen in two ways: in first, called Stokes Raman scattering, the molecule gains energy from the scattered photon, the molecules vibrational level is then increased, as well as having lost some of its energy photons wavelength increases. In the second, called Anti-Stokes Raman scattering, the opposite happens, and the molecule loses some of its vibrational energy to the photon, whose wavelength, in turn, is increased [7]. A comparative image of types of scattering is shown in Figure 1. These both processes in theory have an equal chance of happening, however since most molecules are already at their lowest vibrational level, the Stokes Raman scattering is far more likely to happen and more often measured. In both cases the changes in

the molecules may occur within the vibrational states and rotational states, however if photons with sufficient energy are provided, it may induce fluorescence [6].

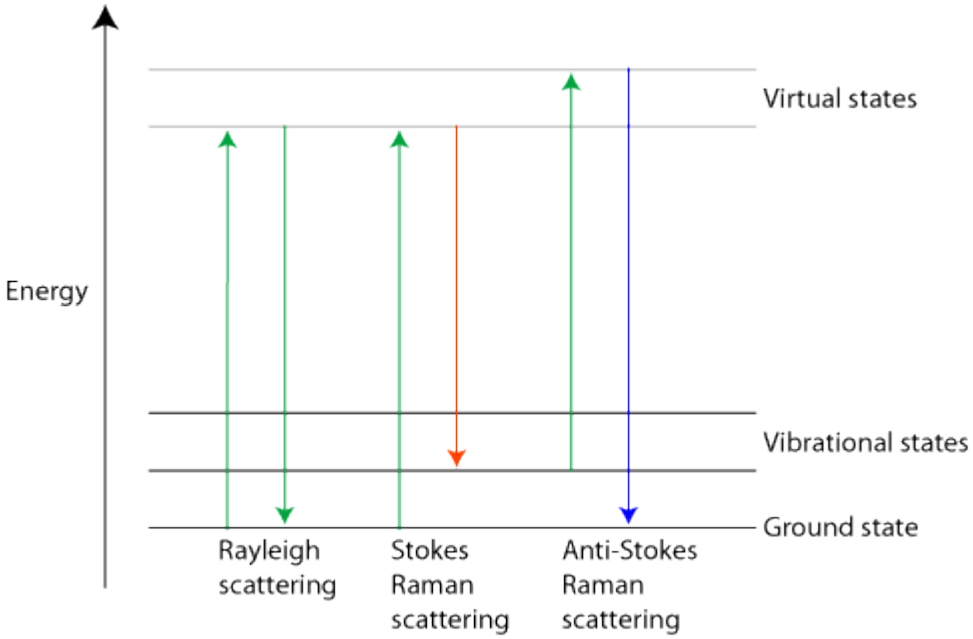

Figure 1. Comparison of types of scattering. *Three different forms of scattering*. University of Cambridge. https://www.doitpoms.ac.uk/tlplib/raman/raman_scattering.php 2004-2020. Accessed 20 May. 2021. The green arrow indicates the virtual energy level reached. In Rayleigh scattering, there are no changes in the energy and vibrational states. In Stokes Raman scattering, the photon loses energy, thus a higher vibration state is achieved by the molecule. In Anti-Stokes Raman scattering, the photon gains energy from the molecule, thus its vibrational state reduces.

1. Attēls. Dažādu gaismas izkliedes tipu salīdzinājums. *Three different forms of scattering*. University of Cambridge. https://www.doitpoms.ac.uk/tlplib/raman/raman_scattering.php 2004-2020. Ņemts 20 maijs. 2021. Zaļā bulta norāda uz virtuālo enerģijas līmeni, kas ir sasniegts. Rayleigh izkliedē nav izmaiņas enerģijas daudzumā un līdz ar to arī vibrācijas līmenī. Stokes Raman izkliedē, fotons zaudē enerģiju molekulai, kas līdz ar to nonāk augstākā energētiskā līmenī. Anti-Stokes Raman izkliedē, fotons iegūst enerģiju no molekulas, kas līdz ar to nonāk zemākā enerģētiskā līmenī.

For a molecule to measurable with Raman spectroscopy, the molecule must pose polarizability, meaning, when subjected to an electromagnetic field, in this case in a form of photons, the molecules electron cloud is distorted, resulting in the formation of a dipole. The atomic bonds between atoms and molecules can then change their relative relation to one another and this, in turn, changes the vibrational and rotational energy [6]. Despite using the properties of polarizability, which is more pronounced in nonpolar molecules, for example, carbon dioxide and benzene, it is possible to measure polar molecules, for example, the polar

amino acids: serine, threonine, and others. As under the influence of an outside electromagnetic field, their poles may still undergo some shifts and changes. Because of this Raman spectroscopy can be referred to as vibrational spectroscopy [7].

Atoms in the molecules have a set number of modes of vibration for example, asymmetric and symmetric stretching, wagging and others. Each mode has a specific energy requirement and thus will produce unique Stokes and Anti-Stokes Raman results [6]. The number of vibrational modes for linear molecules is *3N-5* and for nonlinear *3N-6*, where *N* is the number of atoms in the molecule. It is important to note that not all modes would Raman scatter, due to their symmetry, as well as that overlap between the energies of scattered photons from different molecules is possible, as the size of the molecule increases [7].

The released photon from either Stokes or Anti-Stokes Raman scattering has a specific wavelength, depending on whether the photon gained or lost energy from the electron in the molecule, this new wavelength is specific to corresponding molecules composition, types of chemical bonds, the type of vibrational or rotational changes that have occurred and the number and the type of saturated or unsaturated parts and cyclic compounds [8]. With this it possible to gain insight into the composition and structural fingerprint of the molecules or the samples [9].

Raman spectroscopy can be compared to Infrared spectroscopy, as both methods are a type of vibrational spectroscopy. However, as denoted by its name, infrared spectroscopy uses infrared radiation, while Raman works in the range of visible light, using monochromatic light [10]. Also, infrared spectroscopy works by measuring the absorbed spectra from the sample, instead of the scattered light as in Raman. Another difference is in the atomic bonds that can be measured with each of the systems, as different vibrational types, for example, asymmetric and symmetric stretching, wagging, for the same molecule can be either Raman or infrared spectra inactive, meaning there will be no discernible result. This is mutually exclusive, vibrational modes active in Raman will have little to no activity in infrared and vice versa [10,11]. More often, infrared spectroscopy is used when dealing with asymmetrical molecules, as they have more pronounced electric dipoles, while Raman spectroscopy is used for more symmetric molecule identification [10].

Due to the precise nature of Raman spectroscopy and the ability to assess the chemical composition of the cells and tissues accurately and precisely, this method shows promise as a powerful tool for cancer diagnosis. With precise measurements, specific “fingerprints” or molecular alterations can be detected in the tissues containing cancerous cells[6].

1.2. Raman diagnostical applications

1.2.1. Applications in human medicine

Because of its high chemical specificity and non-invasive nature, Raman spectroscopy has recently been used in several cancer screening and diagnostical applications [5,12]. The progress of Raman based diagnostical applications was hindered by several reasons, such as long data acquisition times, lack of spectra databases and expensive instruments [6]. However, recent years have shown the potential for Raman spectroscopy in cancer research, as it has been used to study a variety of human tissues, such as skin, lung, colon, brain, breast, and others, as well as biofluids, like urine, saliva, and blood [13].

The genetic, phenotypical, and morphological differences of even similar types of cancer present a crucial problem at describing the disease and making any prognosis [14]. Because of this, the identification and development of a large panel of specific, sensitive, and quantitative biomarkers has been the leading task. Furthermore, since classifications based on single or a few biomarkers often fails to provide a correct diagnosis of cancer, the need for a fast, cheap, method to provide a unique and accurate characterization of the cancer is still increasing [5,15] .

Raman spectroscopy is a very promising method for skin cancer detection and characterization, it is one of the most common types of cancer and the incidence is increasing annually. Worldwide in 2020, there were approximately 1.5 million new cases of skin cancer and around 100 thousand deaths [16] . The most common types of skin cancers are Basal cell carcinoma (BCC), Squamous cell carcinoma (SCC) and Melanoma [17]. The most aggressive form of skin cancer: melanoma, while only making up around the third of newly diagnosed cases, contributes contributed half of the patient deaths. Melanoma has a diagnostic accuracy ranging from 49-81% depending on the experience of the dermatologist, equipment, and the amount of tumour available [14]. Moreover, these biopsies might lead to skin lesion progression, are not cost-effective for the patient and the healthcare system and are unpleasant for the patient. Several studies have successfully used Raman spectroscopy to discern different types of skin cancer, as well as to characterize them by their active components [9,18].

Raman spectroscopy applications for skin cancer identification and characterization have been actively studied for more than a decade and progress has been made in developing tools necessary to effectively diagnose skin cancer *in vivo* [5,19]. Several studies have been published on classification methods of skin cancer types using Raman spectra, as well as distinguishing healthy and abnormal tissue, the accuracy and sensitivity often are above 90% [17,20,21].

Sensitivity is the number of correctly identified abnormal tissues and specificity being the number of correctly identified samples without the condition. However, most of these studies are performed *ex vivo,* when performed *in vivo* the results differ, while sensitivity remains above 90%, specificity, on the other hand, varies depending on a specific study between 60-80% [17,19].

The molecular composition and active components of skin cancer have been described and profiled by several authors, several noteworthy changes from normal tissues have been documented [9,20].

- The amount of triolein, a triglyceride that in human skin is present as subcutaneous fats and lipids, is reduced when compared to normal tissue.
- The amount of collagen is lower in nonmelanoma skin cancer than in normal tissue.
- The amount of Elastin is increased in nonmelanoma skin cancer.
- In melanomas, the melanin amount is drastically increased, compared to other skin cancer types and healthy tissues.
- Ribonucleic acid amounts are increased in tumour tissues, compared to normal tissue.

A very important difference noted by several studies is the Amide I band. The Amide I band represents the backbone of the protein geometry and is represented by around 80% C=O bands and roughly 20% C-N bands. Its frequency in a range between 1600 and 1700 cm^{-1} [22]. In normal tissues, the proteins, regulated by the cells, have a particular conformation, content, and amount. In abnormal cells, however, the protein expression is often altered, and this can result in upregulated, inhibited expression or in changed geometry either via incorrect folding or different amino acids. Thus, the Amide I band in tumour tissue shift to a lower wavelength and is broader. Similar findings have been published on Amide band III and lipids; they however are shifted in opposite direction [19,22].

For a complete characterization, these and other parameters are combined, however, the amount of data then increases significantly, with all the variations in all the samples. Because of this various data analysis and statistical methods are often employed. Noteworthy methods used in data analysis are machine learning and neural networks, with these methods research speed is greatly increased as well as automated, easily replicable, they do however require specific training.

Lui *et al.* in 2012 published a clinical study in which different skin cancer types of 453 patients were analysed in vivo. The instrument was set up for an acquisition time of just 1 second and used software to process the data immediately, allowing for real-time skin lesion investigation. The study includes both benign and malignant skin tissues, including BCC, SCC, melanomas, and others less common types of skin cancer, the overall sensitivity of over 95% and specificity in a range from 15% to 54% was achieved. The study managed to distinguish malignant and premalignant disorders from benign, melanomas from benign pigmented skin lesions and melanomas from seborrheic keratoses [17].

Zhang *et al.* in 2018 published a meta-analysis of 12 studies. The Raman spectra were from the chosen studies were pooled into respective groups of *in vivo* and *ex vivo*, and respectively BBC, SCC, and melanomas. The main goal of the study was to assess the sensitivity and specificity of Raman spectroscopy in differentiating skin cancer from normal tissue, Table 1, [23].

Table 1.

Sensitivity and specificity of Raman spectroscopy in differentiating skin cancer from normal tissue (Zhang *et al*. in 2018)

1. Tabula

Ramana spektroskopijas jutīgums un specifiskums, atšķirot ādas vēzi no normāliem audiem (Zhang et al., 2018)

Skin cancer type	*Ex vivo* sensitivity, %	*Ex vivo* specificity, %	*In vivo* sensitivity, %	*In vivo* specificity, %
BCC	99	96	69	85
SCC	96	100	81	98
Melanoma	100	98	93	96

They also note the differences between *in vivo* and *ex vivo* results and attribute them to the limited collection time during the procedure patients would have to be perfectly still for a longer period of time and any movement would decrease the accuracy and quality of the measurements. The study also mention several limitations in the study, such as the need for more Raman spectra data, the number of patients was small, and the number of measurements that differed among selected studies. Also, the majority of the studies used ex vivo tissues and Raman spectroscopy techniques and algorithms in data analysis differed [23].

Nevertheless, the study showed Raman spectroscopy as a very promising tool in skin cancer diagnosis and highlighted some important problems in the field. For example, lack of unified measurement methods, data collection and analysis, and since the current *ex vivo* results are nearing the top, the need for more *in vivo* studies is greatly increasing [23].

1.2.2. Applications in veterinary medicine

Cancer is a very common cause of animal companion deaths, in fact, the leading cause of deaths in canines is cancer, as around 50% of geriatric dogs will die of cancer. As for cats, cancer is the second most common cause of death, with around 33% of cats dying from cancer. This number has increased and is predicted to increase as the advances in veterinary medicine will allow pets to live longer [1,3]. According to several studies, the number of tumours originating from the skin or directly underneath the skin is in a range between 25 to 50% [1,2]. While in the past decade Raman spectroscopy has been used more and more in human medicine, the veterinary field has not seen such advancements.

Currently, the most common approach for cancer detection in pets is based on invasive biopsies, because this method requires for the tumour to be well palpable it works best on larger tumours. During the biopsy, a needle is inserted into the lesion and a tissue sample is taken, to avoid biases the procedure is repeated several times. Because this method is painful the animals often require sedation as not to be a danger to themselves or others, this might create unnecessary complications. In addition, the experience of the veterinarian has a very significant impact on the procedure and its accuracy, which for untrained personnel can vary due to tumours heterogeneous structure and other peculiarities [1,3].

Raman spectroscopy would offer a non-invasive method for benign and malignant tumour detection, that would also be cost-effective and easy to perform. In addition, canine and feline neoplasm studies can serve as an important insight into human neoplasm development, detection, and treatment. Compared to human cats and dogs have a much higher chance to develop tumours. Naturally occurring cat and dog tumours have more similarities to human tumours than any other animal model [3,24].

A number of Raman spectroscopy and animal tumour studies are in relation to breast cancer, because, as mentioned before, the incidence for breast cancer in pets is much higher, while aspects such as age, metastatic pattern, hormonal dependence and genetic and histological characteristics are similar to those in humans [24,25]. A published study in 2020 compared benign and malignant lesions from breast cancer tissues in dogs and showed that the

Raman spectra bands had several similarities with human breast cancer Raman spectra bands [22].

The lack of Raman spectroscopy studies on feline and canine tumour tissues is evident and thus shows the necessity of this study and also creates an opportunity for novel applications and expansion of the field.

2. MATERIALS AND METHODES

2.1.Materials

2.1.1. Samples

The study used 40 tissue samples in total: 4 MCT tissue samples, 9 STS tissue samples and 27 skin tissue samples. Samples were stored in 10% formalin solution. Tumours were identified by pathologist and their precise location marked by small needles.

2.1.2. Apparatus and equipment

Table 2

Used apparatus and equipment.

2. tabula

Izmantotā aparatūra un aprīkojums.

Apparatus	**Description**
784nm diode laser	Cobalt 08-NLD, Hübner, Solna, Sweden.
Imaging spectrometer	iHR320, Horiba, Kyoto, Japan
Shutter control unit	SDRIVE-500, Horiba, Edison, USA.
Laser clean-up filter	LD01-785/10, Semrock, IDEX Health & Science, Rochester, New York, US)
Collection fiber bundle	6 fibers, Ø 400 μm, NA=0.22, Light Guide Optics Germany GmbH, Meckenheim, Germany
Power and Energy Meter	PM100D, Thorlabs, Bergkirchen, Germany

2.1.3. Materials

Table 3

Used consumables.

3. tabula

Izmantotie materiāli.

Materials	**Description**
Parafilma M®	Bemis, ASV
Disposable nitrile gloves	Disposable Nitrile Gloves, ROTH, Karlsruhe, Germany

2.1.4. Software

- “Microsoft Office Excel 2020”;
- “Microsoft Office Word 2020”;
- “USBSpectrometerControl, Version 3.8.1”;
- “LabSpec 6 – HORIBA Scientific, Version 6.4.4.16”

2.1.5. Safety precautions

Formalin was used to preserve tissues, when handling tissue samples it is necessary to exercise caution and wearing protective gloves, eye protection and face mask is a must. As the sample measurement takes a considerable time it is important to ventilate the room. Upon contact with skin immediately wash the area with a large amount of running water as it may cause irritation, sensitivity or a allergic reaction, may also cause serious eye damage.

2.2.Methods

2.2.1. Raman spectrometry

To acquire the Raman spectra of the samples, Raman spectroscopy was performed. The method works by sending a beam of monochromatic light through the sample, the wavelength of the light is changed by Raman scattering and collected by a collector lens and redirected through a notch filter filters out Rayleigh scattered light, then the light is directed towards a diffraction grating, which bends the Raman shifted light according to its wavelength. From there the light is projected onto charged-couple device (CCD) camera. The CCD camera works as photon detector, where photons are absorbed by a special light-sensing element and their energy is transferred to newly released electrons, Figure 2. The resulting charge accumulated in regions is proportional to the number of photons. From there the readout data is produced based on the charge of electrons corresponding to specific wavelength (HORIBA, 2021).

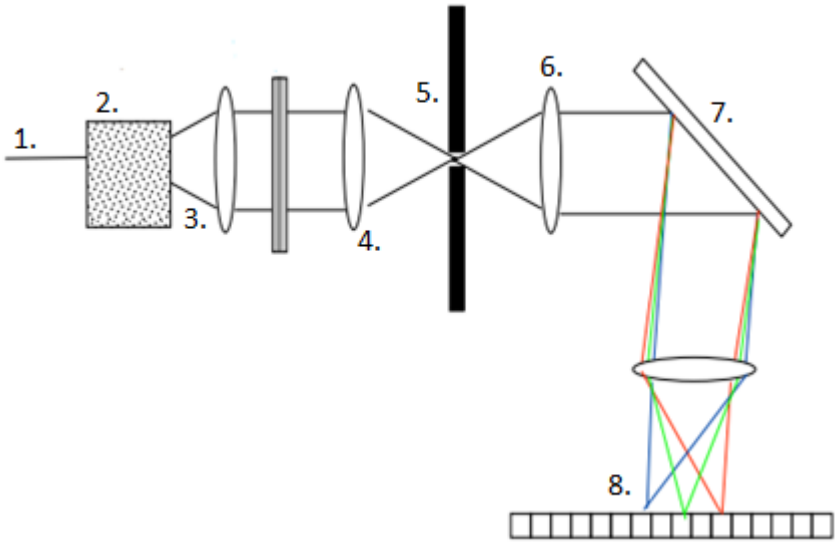

Figure 2. Raman spectrometer components. (Adapted from Thirumalainambi 2005). 1. Initial laser. 2. Sample. 3. Lens for gathering scattered light. 4. Focusing lens. 5. Notch filter. 6. Focusing lens. 7. Diffraction grating. 8. CCD camera.

2.attēls. Raman spektrometra komponentes. (Pārveidots no Thirumalainambi 2005). 1. Sākotnējais lāzers. 2. Paraugs. 3. Objektīvs izkliedētās gaismas savākšanai. 4. Fokusēšanas objektīvs. 5. Iegriezuma filtrs. 6. Fokusēšanas objektīvs. 7. Difrakcijas režģis. 8. CCD kamera.

The sample was placed onto under the laser, unto the measurement platform. Before beginning the measurements run “USBSpectrometerControl, Version 3.8.1” and press “initialize” also the shutter needs to be turned on and opened, both manually and in

“USBSpectrometerControl, Version 3.8.1”. In “LabSpec 6 – HORIBA Scientific, Version 6.4.4.16” set front slit entrance to 50 μm, grating to 1200 and check if laser is set to 785 nm. Run settings are: acquisition time – 90 seconds, accumulation 1, and 300 to 950 cm^{-1}. The detector needs to be cooled and displayed in green. After the measurement it is necessary to remove autofluorescence signal, by performing baseline correction in “LabSpec 6 – HORIBA Scientific, Version 6.4.4.16”, this is done by fitting a polycurve to acquired results and subtracting it. Final step is to remove any cosmic spikes produced by cosmic rays. Cosmic rays are high energy particles from outer space, that, create secondary cosmic rays when entering atmosphere. These rays are random and cannot be avoided, and they create spikes in Raman spectra [26].

3. RESULTS AND DISCUSSION

To better analyse the spectra and avoid any biases, that might have come from sample heterogeneity, each sample was measured 12 times, after each measurement new random location within the marked tumour or skin sample was chosen.

In total 40 samples of tumour tissues and skin were measured, and 480 spectra acquired for the analysis.

3.1. Raman spectra characterization

Raman spectra data for each of the samples was analysed by calculating means and standard deviations of all 12 measurements. Afterwards, for all of the means of the same type of sample new means were calculated along with new standard deviations. These spectra data were then analysed, and spectra bands identified, Table 4. For the specific Raman band peaks, an error of ±7 cm^{-1} was taken into account when characterizing the spectra. This error was included due to Raman spectroscopy resolution which is 7 cm^{-1}.

Table 4

Peak assignments for Raman tissue spectra.

4. tabula

Identificētas Ramana audu spektra virsotnes.

Wavenumber, cm^{-1}	Assigned to
445	Cholesterol, cholesterol ester
538	Cholesterol ester
540	Amino acid: cysteine
548	Cholesterol
614	Cholesterol ester
618	C-C twisting
620	C-C twist aromatic ring
621	C-C twist in phenylalanine
702	Cholesterol, cholesterol ester
717	C-N membrane phospholipids, choline group, lipids
815	Collagen
907	Formalin

3.1.1. MCT spectra characterization

MCT tissue mean Raman spectra characterization in the region from 300 to 950 cm^{-1} showed four cleared and distinct peaks, at 446, 542, 712 and 811 cm^{-1}, Figure 3.

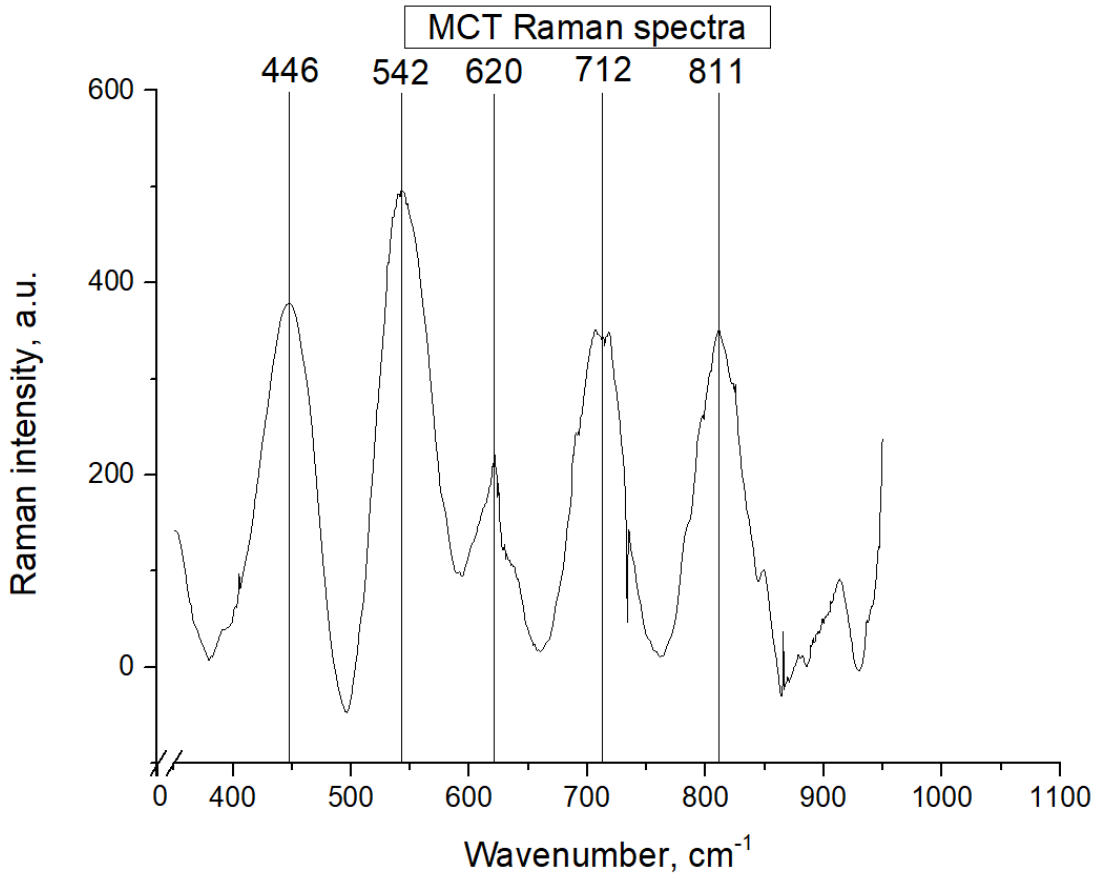

Figure 3. MCT tissue mean Raman spectra, with peak values assigned.

3. attēls. Tuklo šūnu audzēju audu vidējo vērtību Ramana spektrs, ar norādītajām augstākām spectra vērtībām.

The peaks specific peaks correspond to biomolecules and atomic bonds. The 446 cm^{-1} band corresponds to the sample containing cholesterol or cholesterol ester[27,28]. The 542 cm^{-1} band, similarly, also corresponds to cholesterol or cholesterol ester, however, the band may also contain amino acid cysteine, as these ranges overlap[27,28]. Cholesterols presence is to be expected as it is an essential structural lipid, that is important cell membrane component as well participates in a variety of other cellular mechanisms[29]. The 620 cm^{-1} bands presence again is an indication of cholesterol, more interestingly, also of C-C aromatic ring twist and as well as C-C twisting mode of phenylalanine, the C-C aromatic ring is present in a number of organic compounds[28,30]. While the presence of cholesterol in the tissues is understandable, the phenylalanine presence can be explained by the fact that it is a precursor to melanin,

phenylalanine has been detected and described by similar studies[31]. The band in 712 cm^{-1} is related to membrane phospholipids, choline group and lipids, as well as cholesterol[30,31]. The 811 cm^{-1} indicates the presence of collagen within the tissue samples, a structural protein in the extracellular matrix, found in connective tissues[9]. Lastly smaller peak, an unmarked peak at 900 cm^{-1} regions is from formalin, which is from tissue preservation[30].

3.1.2. STS spectra characterization

After analysis, the overall STS mean Raman spectra showed great similarity to MCT spectra, Figure 3. and 4.

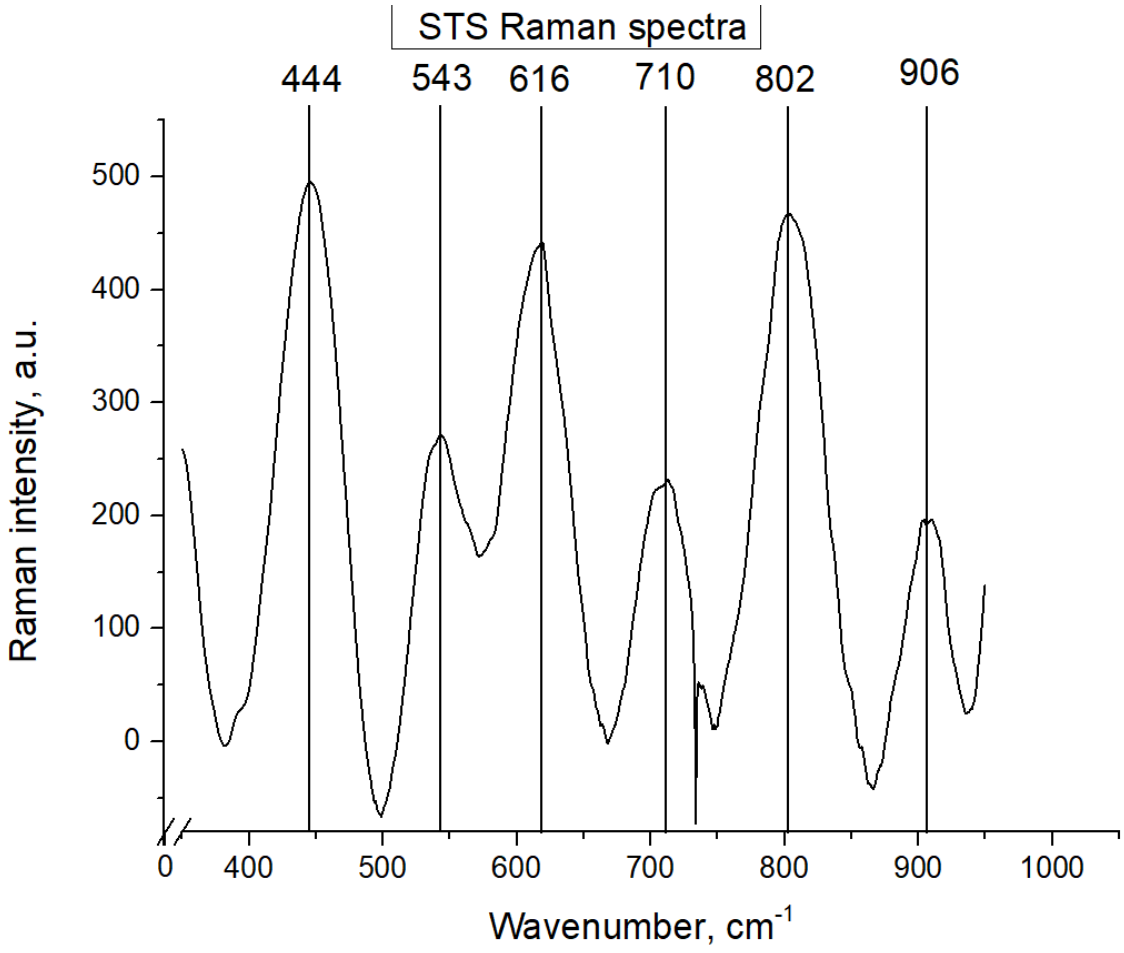

Figure 4. STS tissue mean Raman spectra, with peak values assigned.

4. attēls. Mīksto audu sarcomu audu vidējo vērtību Ramana spektrs, ar norādītajām augstākām spectra vērtībām.

Despite the different origin of the tumours, STS stem from mesenchymal cells and MCT originate from the bone barrow. STS Raman spectra produced six distinct spectral regions, including 906 cm^{-1}, which is formalin produced band. The 444, 543, 616, 710 cm^{-1}

correspond to the presence of cholesterol[27]. The 543 cm^{-1} band can also be a result of cysteine[30]. 616 cm^{-1} band can be produced by phenylalanine C-C bond twisting and C-C aromatic ring twisting in molecules[28,30]. 710 cm^{-1} stem from membrane phospholipids and lipids[27]. Lastly, the 802 cm^{-1} band again is the result of collagen in the tissue sample[9].

3.1.3. Raman spectra comparison

The mean spectra of MCT, STS and skin tissue samples were compared among each other and the results are shown in, Figure 5. The STS tissues showed increasing Raman band intensity at 445, 619 and 803 cm^{-1} regions, the 907 cm^{-1}, which has been omitted as the band is produced by formalin. These results would indicate that STS could have increased amounts of cholesterol that would produce bands of higher intensity[27]. As the 619 cm^{-1} band is also produced by cysteine, it could be an indicator of increased specific amino acid content[30]. While the 803 cm^{-1} band shows differences in the band relating to collagen Raman scattering[9].

MCT tissues showed the most intense peak at 541 cm^{-1}, which corresponds to cholesterol, C-C phenylalanine twisting and C-C aromatic ring twisting[27,30]. The 713 cm^{-1} also shows a peak with a more pronounced MCT peak, as mentioned before, this peak can be produced by membrane phospholipids, lipids and the choline group. As for skin tissues, overall, the spectra was less intense than that of the tumour tissues, this could be due to skin tendency to absorb more light, so less of it is scattered when compared to deeper located tumour tissues[32].

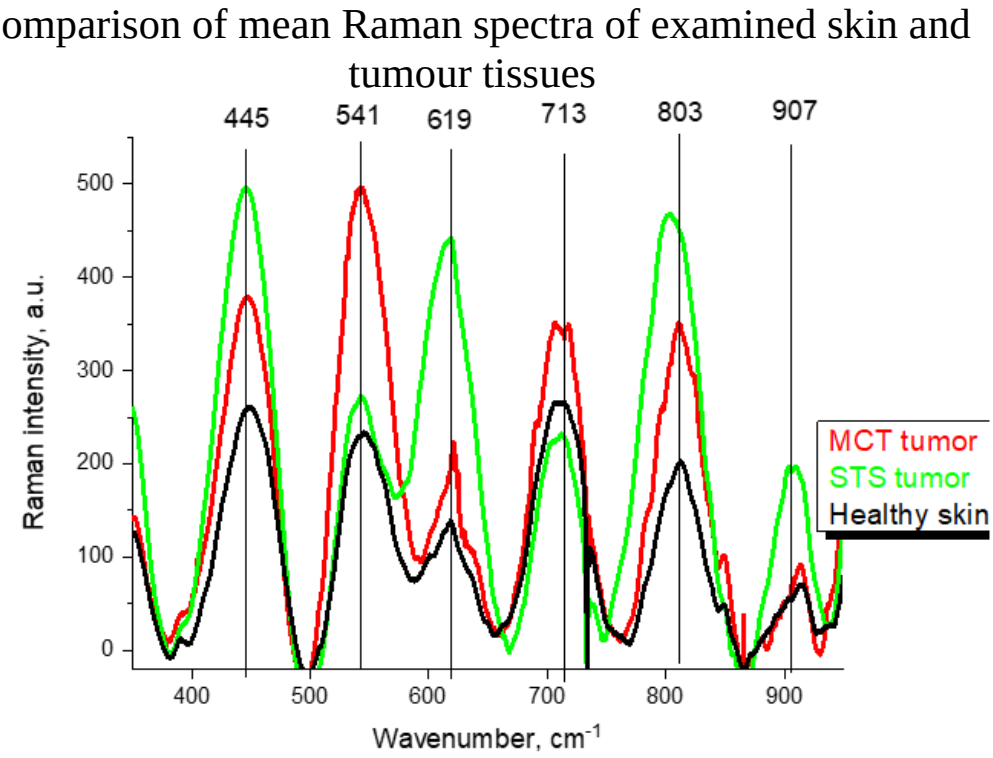

Figure 5. Comparison of mean Raman spectra of examined skin and tumour tissues

5. attēls. Ādas un audzēja audu vidējo Ramana spektru salīdzinājums

3.2. Principal component analysis

The principal component analysis (PCA) is used to identify the most significant variances in the tissue spectra and to classify the tissues by type. As for multivariate data analysis, the method works by reducing the dimensionality of large sets of data, as in the case of Raman spectral data. The result is a smaller set of data that can be more easily visualized and analysed[33].

The loading plots of two principal components (PC) in the range from 300 to 950 cm^{-1} are shown in Figure 6. The loading varies in the range from -1 to 1, and the closer a variable is to this value more strongly it influences the component and shows how significant variance was in each part of the Raman spectra[33].

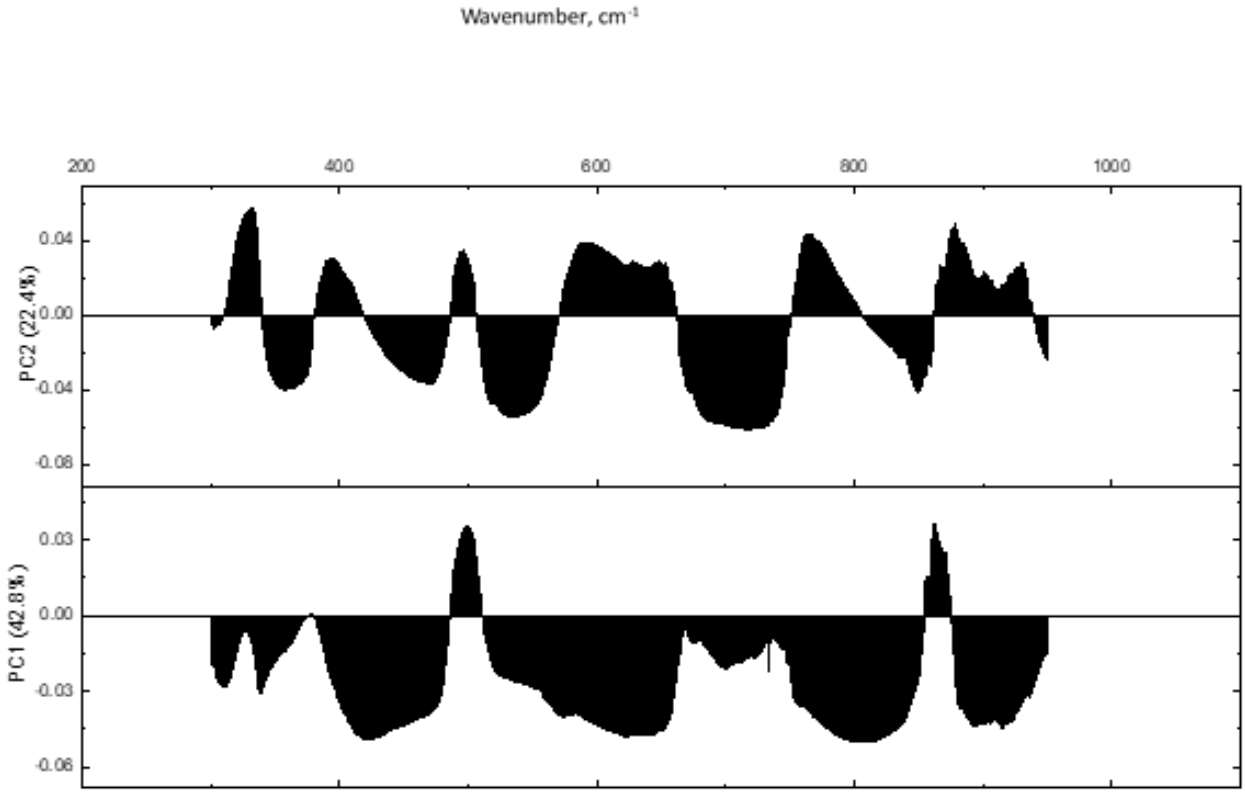

Figure 6. Loading plot of PC1 and PC2.

6. attēls. “Loading plot” priekš PK1 un PK2

A score plot is a PCA model, which uses the two most significant variables and displays them in a graph. Figure 7 shows the first two principal components, which includes 65.2% of all spectral variations. Each square represents a tissue sample, and they are clustered by their relation to one another. The dotted line was manually drawn to separate between as many skin and tumour tissue samples. Even though MCT and STS could not be distinguished by PCA, the majority of tumour and skin tissues can be separated into categories depending on the PC1 and PC2 scores.

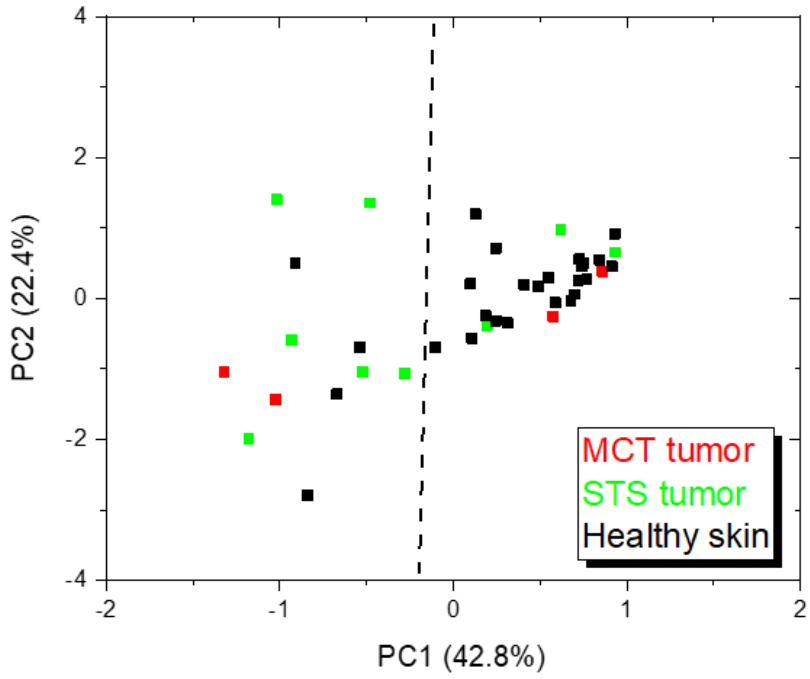

Figure 7. Score plot of PC1 and PC2.

7. attēls. "Score plot" priekš PK1 un PK2

The poor separation could be because of the small tumour sample size, as only 4 MCT and 9 STS were used in the study. However, it might also be that the selected spectral range 300-950 cm^{-1} is not suitable for very precise diagnostic operations, as almost all of the spectra characteristics significantly overlapped between STS, MCT and to a lesser extent also skin tissue samples.

In order to further check this spectra range as a diagnostic tool for tumours specificity and sensitivity were calculated from the results of the PCA score plot, Table 5.

Table 5

Results of tissue discrimination in PCA.

5. tabula

PKA audu identificēšanas rezultāti

	Raman		
Histopathology (gold standart)	Skin	Tumours	
Skin (n = 27)	23 (TN)	5 (FP)	
Tumours (STS, n = 9)	4 (FN)	8 (TP)	
(MCT, n = 4)			
Skin vs Tumours	Sensitivity = TP/(TP+FN) =66.6 %	Specificity = TN/(TN+FP) = 82.1%	Accuracy = 77.5 % = ((TP+TN)/(TN+FP+FN+TN))

The sensitivity means the number of skin tissue samples that were correctly identified as skin, TN meaning true negative and FN meaning false negative. This means that sensitivity is only 66.6%. The specificity means the number of tumour samples that were correctly identified as tumours, FP meaning false positive and TP meaning true positive. The gold standard used for here is the histopathological information provided by the professional histopathologist.

Possible reasons for the low results could be due to the small sample size, slight variations between MCT and STS tissues, and possibly due to histological differences between feline and canine cells.

3.3. Data analysis with spectra normalization

As the spectral data among measurements in each sample and same types of tissues showed a significant variation, Appendix 1. In order to reduce the large differences in the ranges of initial variables standardization was performed. Several studies have shown the need to normalize the data to achieve better PCA results[20,21,12].

Mean normalized Raman spectra of STS, MCT and skin tissue samples is shown in Figure 8. The range of the standard deviation for MCT is shown in light red, STS - light green, skin – grey.

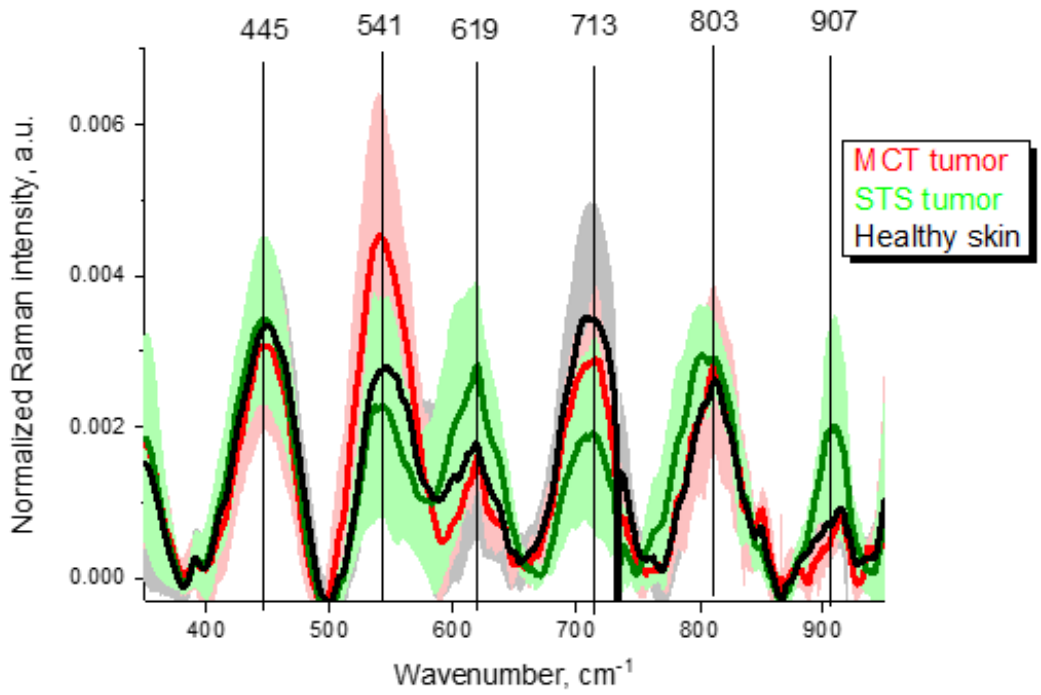

Figure 8. Mean normalized Raman spectra of STS, MCT and skin tissue samples

8. attēls. STS, MCT un ādas audu paraugu vidējie normalizētie Ramana spektri

When compared to nonnormalized mean Raman spectra data the normalized graph shows less distinction between the spectra, as 445 and 803 cm^{-1} are overlapping. However, it is important to note that skin samples showed significantly smaller variation, while STS and MCT Raman intensity has been greatly reduced. A possible cause for this might have been the low tumour tissue sample amount, as fewer number of measurements would show a greater variation amongst themselves than many.

With the normalised Raman spectra data PCA was repeated, Figure 9. Compared to nonnormalized data the samples, especially skin, showed reduced clustering. However, the analysis was still unable to separate MCT and STS tissue samples, the differentiation between tumour and skin samples was at a similar level.

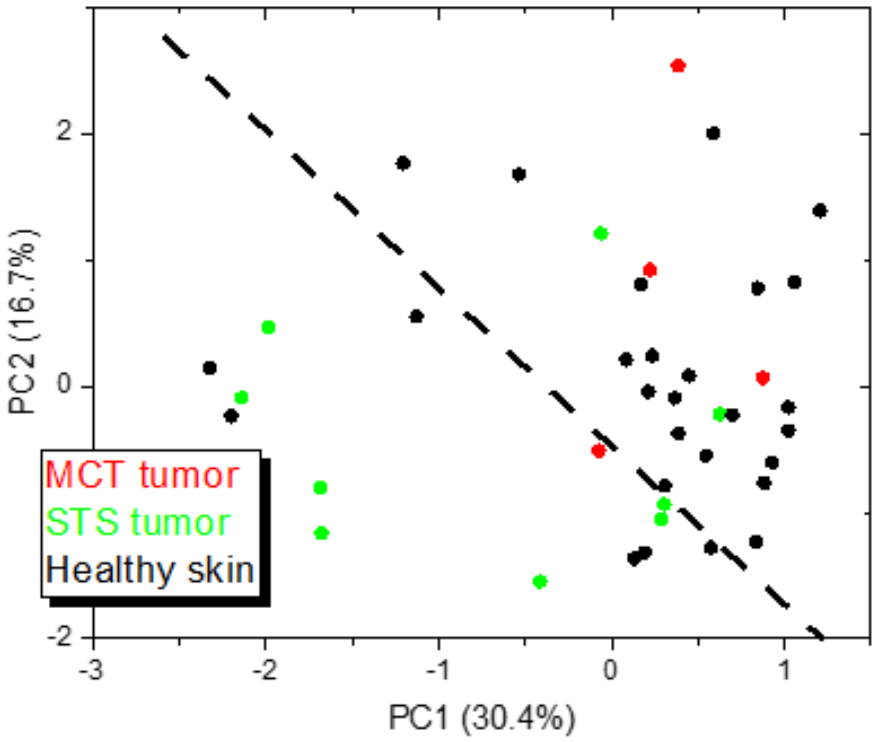

Figure 9. The scatter plot of PC1 and PC2 from normalized Raman spectra.

9. attēls. PK1 un PK2 "Scatter plot" no normalizētām Ramana spectra vērtībām.

Table 6 shows the sensitivity, specificity, and accuracy of PCA on normalized spectra. Tissue discrimination is compared between the spectral regions on this study (300-950 cm^{-1}) and a study performed with the same samples within 950-2050 cm^{-1} spectral regions [34]. When comped to nonnormalized Raman spectra data, the normalized spectra show reduced sensitivity, from 66.6% to 57.1%. Specificity, however, has had a slight increase, from 82.1% to 88.2%. But the accuracy has slightly decreased, from 77.5% to 72.5%. Nevertheless, in both cases, the 300-950 cm^{-1} range shows a significantly worse performance in accurately diagnosing tumour and skin tissue samples when compared to the 950-2050 cm^{-1} range. As the studies showed 100% sensitivity, 88.2% specificity and 95.5% accuracy.

While the results in this study might be slightly attributed to the ratio of tumour and tissue samples used for analysis, it is, however, unlikely, as the spectra characterization showed large similarities. As mentioned before a possible way to improve the overall diagnosis results could be by increasing the number of total samples. Also, possibly separating the samples by

species might provide some insight into their characteristics, however with the current sample size that is not feasible.

Table 6

Results of tissue discrimination in PCA with normalised Raman tissue spectra.

6. tabula

PKA audu identificēšanas rezultāti ar normalizētām Ramana spektra vērtībām

	Raman		
Histopathology	Skin	Tumors	
(gold standard)	300 – 950 (950 – 2050) cm^{-1}	300 – 950 (950 – 2050) cm^{-1}	
Skin (n = 27)	21 (15)	5 (2)	
Tumors (STS, n = 9)	6 (0)	8 (28)	
(MCT, n = 4)			
Skin vs Tumors	Sensitivity = 57.1 %	Specificity = 80.7 %	Accuracy = 72.5 %
	(Sensitivity = 100 %)	(Specificity = 88.2 %)	Accuracy = 95.5 %

CONCLUSIONS

1. The obtained spectral analysis data, after their characterization, coincide with those previously described in the literature, however between the samples showed little variation.
2. After the PCA, the sensitivity, specificity and accuracy in this spectral range are lower than for the corresponding samples within a different spectral range, which indicates that the selected spectrum is not suitable for cancer diagnosis.

ACKNOWLEDGEMENTS

I express my gratitude to, the supervisor of the bachelor thesis for the advice has has given during the process of making it, as well as for correcting and editing it. As well as for the opportunity to develop the bachelor thesis at the Institute of Atomic Physics and Spectroscopy / Biophotonics Laboratory of the University of Latvia

My thanks to Daira Viškere for the information about the samples.

BIBLIOGRAPHY

1. Withrow SJ. *Why Worry About Cancer in Pets?* Vol 53. Fourth Edi. Elsevier Inc.; 2013. doi:10.1016/B978-0-7216-0558-6.50003-4

2. Baioni E, Scanziani E, Vincenti MC, et al. Estimating canine cancer incidence: findings from a population-based tumour registry in northwestern Italy. *BMC Vet Res*. 2017;13(1):203. doi:10.1186/s12917-017-1126-0

3. Hauck ML. *Tumors of the Skin and Subcutaneous Tissues*. Fifth Edit. Elsevier Inc.; 2012. doi:10.1016/B978-1-4377-2362-5.00018-9

4. Cordero E. In-vivo Raman spectroscopy: from basics to applications. *J Biomed Opt*. 2018;23(07):1. doi:10.1117/1.jbo.23.7.071210

5. Austin LA, Osseiran S, Evans CL. Raman technologies in cancer diagnostics. *Analyst*. 2016;141(2):476-503. doi:10.1039/c5an01786f

6. Jones RR, Hooper DC, Zhang L, Wolverson D, Valev VK. Raman Techniques: Fundamentals and Frontiers. *Nanoscale Res Lett*. 2019;14(1). doi:10.1186/s11671-019-3039-2

7. Chaudhuri D. Theoretical aspects. *Xinjiang and the Chinese State*. 2018:37-59. doi:10.4324/9780203732168-3

8. Yorucu C. Raman analysis of tissue engineered normal skin and melanoma. 2015;(August).

9. Feng X, Moy AJ, Nguyen HTM, et al. Raman active components of skin cancer. *Biomed Opt Express*. 2017;8(6):2835. doi:10.1364/boe.8.002835

10. Beć KB, Grabska J, Huck CW. Biomolecular and bioanalytical applications of infrared spectroscopy – A review. *Anal Chim Acta*. 2020;1133:150-177. doi:10.1016/j.aca.2020.04.015

11. Hassing S. What Is Vibrational Raman Spectroscopy: A Vibrational or an Electronic Spectroscopic Technique or Both? *Mod Spectrosc Tech Appl*. 2020:1-25. doi:10.5772/intechopen.86838

12. Brauchle E, Noor S, Holtorf E, Garbe C, Schenke-Layland K, Busch C. Raman spectroscopy as an analytical tool for melanoma research. *Clin Exp Dermatol*. 2014;39(5):636-645. doi:10.1111/ced.12357

13. Auner GW, Koya SK, Huang C, et al. Applications of Raman spectroscopy in cancer diagnosis. *Cancer Metastasis Rev*. 2018;37(4):691-717. doi:10.1007/s10555-018-9770-9

14. Shannan B, Perego M, Somasundaram R, Herlyn M. Heterogeneity in Melanoma. In: ; 2016:1-15. doi:10.1007/978-3-319-22539-5_1

15. Gniadecka M, Philipsen PA, Sigurdsson S, et al. Melanoma Diagnosis by Raman Spectroscopy and Neural Networks: Structure Alterations in Proteins and Lipids in Intact Cancer Tissue. *J Invest Dermatol*. 2004;122(2):443-449. doi:10.1046/j.0022-202X.2004.22208.x

16. Global Cancer Observatory. *Global Cancer Burden 2020.*; 2020.

17. Lui H, Zhao J, McLean D, Zeng H. Real-time raman spectroscopy for in vivo skin cancer diagnosis. *Cancer Res*. 2012;72(10):2491-2500. doi:10.1158/0008-5472.CAN-11-4061

18. Gniadecka M, Wulf HC, Mortensen NN, Nielsen OF, Christensen DH. Diagnosis of basal cell carcinoma by Raman spectroscopy. *J Raman Spectrosc*. 1997;28(2-3):125-129. doi:10.1002/(sici)1097-4555(199702)28:2/3<125::aid-jrs65>3.0.co;2-#

19. Lieber CA, Majumder SK, Ellis DL, Billheimer DD, Mahadevan-Jansen A. In vivo nonmelanoma skin cancer diagnosis using Raman microspectroscopy. *Lasers Surg Med*. 2008;40(7):461-467. doi:10.1002/lsm.20653

20. Baek SJ, Park A, Kim JY, Na SY, Won Y, Choo J. Detection of basal cell carcinoma by automatic classification of confocal Raman spectra. *Lect Notes Comput Sci (including Subser Lect Notes Artif Intell Lect Notes Bioinformatics)*. 2006;4115 LNBI:402-411. doi:10.1007/11816102_44

21. Bodanese B, Silveira FL, Zĝngaro RA, Pacheco MTT, Pasqualucci CA, Silveira L. Discrimination of basal cell carcinoma and melanoma from normal skin biopsies in vitro through raman spectroscopy and principal component analysis. *Photomed Laser Surg*. 2012;30(7):381-387. doi:10.1089/pho.2011.3191

22. Dantas D, Soares L, Novais S, et al. Discrimination of benign and malignant lesions in canine mammary tissue samples using Raman spectroscopy: A pilot study. *Animals*. 2020;10(9):1-16. doi:10.3390/ani10091652

23. Zhang J, Fan Y, Song Y, Xu J. Accuracy of Raman spectroscopy for differentiating

skin cancer from normal tissue. *Medicine (Baltimore)*. 2018;97(34):e12022. doi:10.1097/MD.0000000000012022

24. Birtoiu IA, Rizea C, Togoe D, et al. Diagnosing clean margins through Raman spectroscopy in human and animal mammary tumour surgery: a short review. *Interface Focus*. 2016;6(6):20160067. doi:10.1098/rsfs.2016.0067

25. LeBlanc AK, Breen M, Choyke P, et al. Perspectives from man's best friend: National Academy of Medicine's Workshop on Comparative Oncology. *Sci Transl Med*. 2016;8(324):324ps5-324ps5. doi:10.1126/scitranslmed.aaf0746

26. Li S, Dai L. An Improved Algorithm to Remove Cosmic Spikes in Raman Spectra for Online Monitoring. *Appl Spectrosc*. 2011;65(11):1300-1306. doi:10.1366/10-06169

27. Krafft C, Neudert L, Simat T, Salzer R. Near infrared Raman spectra of human brain lipids. *Spectrochim Acta Part A Mol Biomol Spectrosc*. 2005;61(7):1529-1535. doi:10.1016/j.saa.2004.11.017

28. Stone N, Kendall C, Smith J, Crow P, Barr H. Raman spectroscopy for identification of epithelial cancers. *Faraday Discuss*. 2004;126(1):141-157. doi:10.1039/b304992b

29. Zampelas, Magriplis. New Insights into Cholesterol Functions: A Friend or an Enemy? *Nutrients*. 2019;11(7):1645. doi:10.3390/nu11071645

30. Movasaghi Z, Rehman S, Rehman IU. Raman spectroscopy of biological tissues. *Appl Spectrosc Rev*. 2007;42(5):493-541. doi:10.1080/05704920701551530

31. Stone N, Kendall C, Shepherd N, Crow P, Barr H. Near-infrared Raman spectroscopy for the classification of epithelial pre-cancers and cancers. *J Raman Spectrosc*. 2002;33(7):564-573. doi:10.1002/jrs.882

32. Baranoski GVG, Krishnaswamy A. An Introduction to Light Interaction with Human Skin. *Rev Informática Teórica e Apl*. 2004;11(1):33-62. doi:10.22456/2175-2745.5961

33. Jolliffe IT, Cadima J. Principal component analysis: a review and recent developments. *Philos Trans R Soc A Math Phys Eng Sci*. 2016;374(2065):20150202. doi:10.1098/rsta.2015.0202

34. Cugmas B, Viškere D, Čiževskis O, Melderis M, Rubins U, Tamosiunas M. Optical coherence tomography and Raman spectroscopy for ex vivo characterization of canine skin and subcutaneous tumors: preliminary results. 2021;1(1):9.

doi:10.1117/12.257875

APPENDICES

Appendix 1

Mean spectra of each of tissue types from all of the samples unpoled, indicating variation among the Raman spectral values.

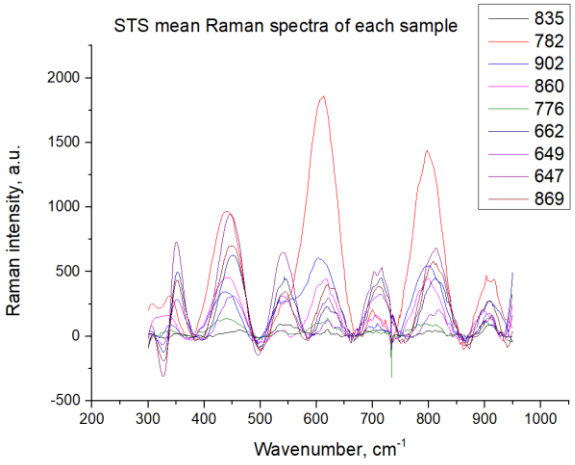

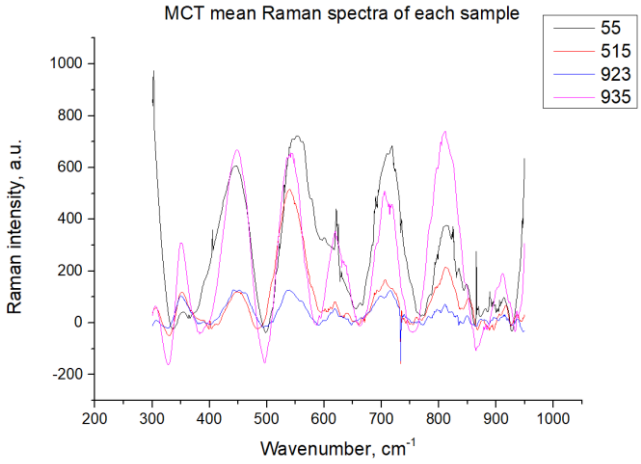

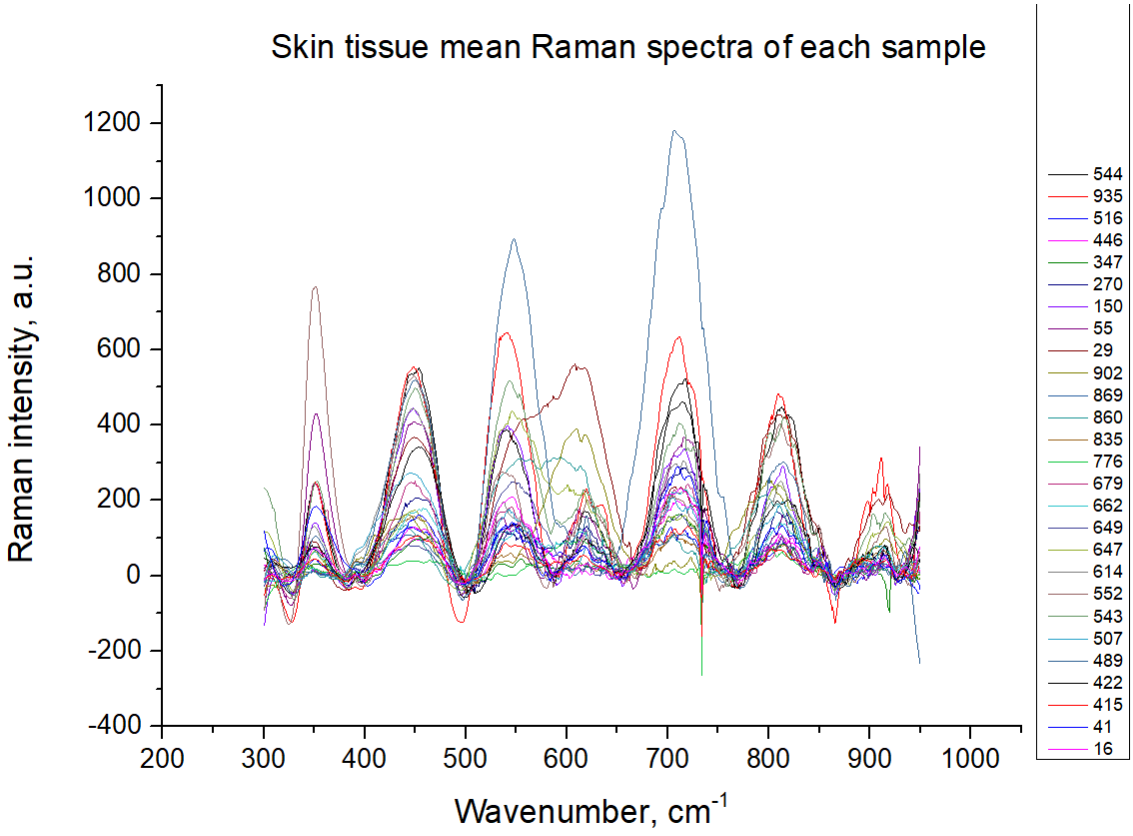

Bakalaura darbs „Subcutaneous canine and feline neoplasm *ex vivo* characterization using Raman spectroscopy” izstrādāts LU Atomfizikas un spektroskopijas institūtā.

Ar savu parakstu apliecinu, ka pētījums veikts patstāvīgi, izmantoti tikai tajā norādītie informācijas avoti un iesniegtā darba elektroniskā kopija atbilst izdrukai.

Autors: Mikus Melderis *paraksts* 28.05.2021.

Rekomendēju darbu aizstāvēšanai

Vadītājs: Dr.phys Mindaugas Tamošiūnas *paraksts* 28.05.2021.

Recenzents: *paraksts* Dr.phys Blaz Cugmas

Darbs iesniegts LU Bioloģijas fakultātē 28.05.2021.

Lietvede: …… *paraksts*

Darbs aizstāvēts Bioloģijas bakalaura gala pārbaudījuma komisijas sēdē

prot. Nr. , vērtējums

Komisijas sekretārs/e: